Modeling and simulation of the tool wear in nanometric cutting

K. Cheng, X. Luo and R. Holt, Modelling and simulation on the tool wear in nanometric cutting, WEARVolume 255, Number 7, August 2003 , pp. 1427-1432(6)

K. Cheng*, X. Luo, R. Ward and R. Holt

School of Engineering, Leeds Metropolitan University, Calverley Street, Leeds LS1 3HE, UK

Abstract

Tool wear is a significant factor affecting the machined surface quality. In this paper, a Molecular Dynamics (MD) simulation approach is proposed to model the wear of the diamond tool in nanometric cutting. It includes the effects of the cutting heat on the workpiece property. MD simulation is carried out to simulate the nanometric cutting of a single crystal silicon plate with the diamond tip of an Atomic Force Microscope (AFM). The wear mechanism is investigated by the calculation of the temperature, the stress in the diamond tip, and the analysis of the relationship between the temperature and sublimation energy of the diamond atoms and silicon atoms. Microstrength is used to characterize the wear resistance of the diamond tool. The machining trials on an AFM are performed to validate the results of the MD simulation. The results of MD simulation and AFM experiments all show that the thermo-chemical wear is the basic wear mechanism of the diamond cutting tool.

Key words: Nanometric cutting, Molecular Dynamics, Tool wear, AFM

Correspondence to: Prof. Kai Cheng, School of Engineering, Leeds Metropolitan University, Calverley Street, Leeds LS1 3HE, UK
TEL: 0113 283 6731 FAX: 0113 283 3110 E-mail: K. Cheng@lmu.ac.uk

1. Introduction

Diamond tools are used extensively in nanometric cutting. The wear of a diamond tool during the machining degrades the machined surface roughness to some extent before the tool failure [1], it will also damage the condition of the machined surface, i.e. the surface integrity [2]. The performance of a precision component or product not only depends on its surface finish but also depends on its surface integrity. Therefore, it is of great significance to get better understanding of the physical aspects of the wear of the diamond cutting tool.

In nanometric cutting processes, the interatomic actions within the surface and subsurface layers will become dominant. Since the 1980s, Molecular Dynamics (MD) simulation has been employed to study nanometric cutting from the point of view of atomic structure. Belak and Hoover in LLNL and Ikawa and Shimada in Japan are the pioneers of this study [3][4], they have investigated the effect of cutting edge radius and minimum cut thickness in the nanometric cutting process. Inamura in Japan built a model that combined FEM and MDS [5], Rentsch in Germany and Komanduri in USA studied the crystallographic orientation effects on nanometric cutting processes [6][7]. Komanduri et al. also investigated the anisotropy and friction by MD simulation of indentation and scratching of single crystal aluminum [8]. A sound foundation has been laid, but all their work did not involve the tool wear. Although Maekawa et al. [9] postulated Morse type potentials with various magnitudes of the cohesion energy to approximate the friction and tool wear, the postulation needs experimental validation. The development of Atomic Force Microscope (AFM) techniques provide a powerful tool for the experimental validation. The sharp diamond tip of AFM can be used to emulate the single-point diamond cutting tool in cutting the workpiece surface [10].

In this paper, the effects of cutting heat on the variation of workpiece property are thoroughly investigated with a MD simulation based on the Modified Embedded Atom Method (MEAM). The simulation is performed to simulate the tool wear in nanometric cutting of single crystal silicon

Correspondence to: Prof. Kai Cheng, School of Engineering, Leeds Metropolitan University, Calverley Street, Leeds LS1 3HE, UK
TEL: 0113 283 6731 FAX: 0113 283 3110 E-mail: K. Cheng@lmu.ac.uk

using the AFM diamond tip. Nanometric cutting experiments using the AFM diamond tip are carried out to evaluate and validate the simulation results.

2. **Nanometric cutting model**

2.1 MD model of the nanometric cutting

The MD model of the nanometric cutting using the AFM diamond tip is shown in Fig.1. The triangular based pyramid shape of the diamond tip is consistent with that of the real AFM diamond tip, but its scale is one thirtieth of the real size of the AFM diamond tip to reduce the computation time. The cone angle (the angle between the cutting edge and its opposite side face) of the diamond tip is 90˚. The cutting edge radius is 1 nm. A single crystal silicon plate is the workpiece. The workpiece is divided into three different zones, namely the Newton atoms zone, the thermostatic atoms zone and the boundary atoms zone. The boundary atoms are assumed to be unaffected by the indentation and scratching process. Consequently, they are fixed in their initial lattice positions and serve to reduce the boundary effects and maintain the proper symmetry of the lattice. The motions of the thermostatic atoms are modified by the method of velocity reset [11]. This procedure is used to simulate the thermostatic effects of the bulk and guarantee the equilibrium temperature to approach the desired value since much of the cutting heat converted from elastic/shear energy and friction energy will be carried away by chip and lubricant in actual machining. The motions of the atoms in the Newton atoms zone and the AFM diamond tip are determined by the interatomic forces produced by the interaction potential and direct solution of Newton’s motion equation. Thus, the interactions between the workpiece and the AFM diamond tip can be studied using this approach. The dimension of the Newton atoms zone is 5.99 nm (length) × 1.18 nm (width) × 3.64 nm (height). The reason to choose a small size of silicon plate is to reduce the simulation time. The initial positions of work atoms and diamond tip atoms are the sites on their crystal lattice. Their initial velocities can be assigned from the Maxwell distribution at 298K.

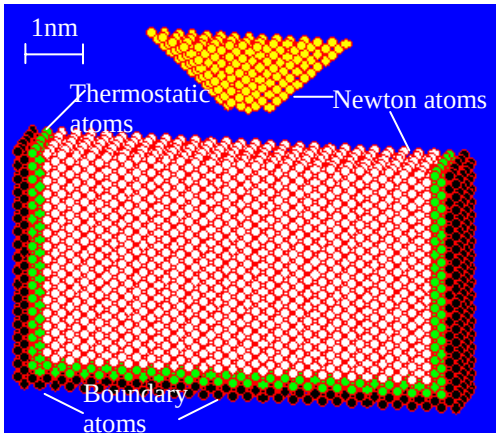

Fig. 1. MD model of Nanometric cutting.

2.2 Modeling of tool wear

From a microscopic point of view, tool wear is the result of interactions between the workpiece atoms and the cutting tool atoms. It can be modelled on condition that the interactions can be described more accurately. In this research, the effect of cutting heat is included in the MD simulation to model and simulate the tool wear.

Generally, the interatomic forces between the workpiece atoms and tool atoms can be calculated by the difference of their respective potential energy. Here, the MEAM potential developed by Professor Baskes [12] is employed, i.e. the potential energy of the *i*-th atom is:

$$E_i = \frac{1}{Z_i}\sum_{j(\neq i)} E_s(r_{ij}) + [F_i(\frac{\rho_i}{Z_i}) - \frac{1}{Z_i}\sum_{j(\neq i)} F_i(\frac{\overline{\rho}_i(r_{ij})}{Z_i})] \quad (1)$$

where E_s, F, Z_i, r_{ij} are the energy per atom of the reference structure, a functional of electron density, the number of the nearest neighbors of the *i*-th atom, the distance between the *i*-th atom and the *j*-th atom, respectively. The reference structure is the equilibrium crystal structure of the atoms. ρ_i and $\overline{\rho}_i$ are the electron density of the real lattice and the reference lattice respectively. This equation has an appealing physical interpretation. The first term in Eq. (1) is simply the average of the energy per atom of the reference lattice at each of the nearest-neighbor distances. The second term is formed by the difference between the embedding energy at the background electron density actually seen by atom *i* and the average embedding energy of this atom in the reference lattice at each of the nearest-neighbor distances [12]. The energy of an element in the reference structure is given by a universal energy function:

$$E_s = -E_{sub}(1+a^*)e^{-a^*} \quad (2a)$$

$$a^* = a_i(R/R_i^0 - 1) \quad (2b)$$

$$a_i = \sqrt{9B_i\Omega_i / E_{sub}} \quad (2c)$$

where R_i^0 is the equilibrium nearest-neighbor distance, B_i is the bulk modulus, Ω_i is the atomic volume of the solid elements, and E_{sub} is the sublimation energy.

It is noted that the sublimation energy is related to the temperature of the system. In order to analyze the tool wear mechanism, it is postulated that the cutting energy is completely transformed into the cutting heat, which results in a rise of cutting temperature. The equilibrium temperature of the system is calculated by the theorem of equipartition of energy, and then the enthalpy of sublimation by Kirchhoff's law:

$$\Delta_s^g H(T_2) = \Delta_s^g H(T_1) + \int_{T_1}^{T_2} [C_p(g) - C_p(s) dT \tag{3}$$

where $\Delta_s^g H(T_1)$ and $\Delta_s^g H(T_2)$ are the enthalpy of sublimation at temperature T_1 and temperature T_2 under standard atmospheric pressure, respectively. $C_p(g)$ and $C_p(s)$ are the heat capacities at constant pressure of the gas and the solid state, respectively. In this canonical ensemble due to the constant pressure, the enthalpy of sublimation equals to sublimation energy. Therefore, the sublimation energy in Eq. (2a) is rectified in the light of the temperature. Because the difference of potential energy is the interatomic force, the cutting heat is then transformed into load force. The forces acting on the *i*-th workpiece silicon atom is

$$F_{wi} = \sum_{j \neq i}^{N_t} F_{wtij} + \sum_{j \neq i}^{N_w} F_{wwij} = \sum_{j \neq i}^{N_t} - \frac{dE_{wti}(r_{wtij})}{dr_{wtij}} + \sum_{j \neq i}^{N_w} - \frac{dE_{wwi}(r_{wwij})}{dr_{wwij}} \tag{4}$$

where E_{wti} and E_{wwi} are the potentials of the *i*-th workpiece atom under the action of diamond tip atoms and other workpiece atoms respectively. N_t, N_w are the number of diamond tip atoms and workpiece atoms respectively. r_{wtij} and r_{wwij} are the distance between the *i*-th workpiece atom and diamond tip atoms and other workpiece atoms respectively. The equation of the forces acted on the *i*-th diamond tip atom is very similar to Eq. (4). Its derivation is omitted because of the limitation of the number of pages. According to the Newton's second law, the movements of the Newton atoms and thermostatic atoms of the workpiece and diamond tip atoms are expressed as:

$$m_{wi}\ddot{r}_{wi} = F_{wi}(r_{wwij}, r_{wtij}) \qquad (i=1, 2,\ldots, N_w) \tag{5}$$

$$m_{ti}\ddot{r}_{ti} = F_{ti}(r_{twij}, r_{ttij}) \qquad (i=1, 2,\ldots, N_t) \tag{6}$$

where r_{wi} and r_{ti} are the displacement vector of workpiece material atoms and cutting tool atoms respectively. r_{ttij} and r_{twij} are the distance between the i-th diamond tip atom and other diamond tip atoms and workpiece atoms respectively. The Euler algorithm can be used to solve these functions, and the result will be the displacement and the velocity of the individual workpiece and diamond tip atoms in the cutting zone. The tool wear can therefore be studied by analysing the loci of these atoms.

3. Tool wear simulation

3.1 The observation of tool wear

In the simulation, the (110) plane is chosen as the rake face and flank face of the AFM diamond tip. The AFM diamond tip is indented into the (001) plane of the workpiece with a speed about 10 m/s. The indentation and scratching depth is set at 0.94 nm. The scratching is carried out along the <010> direction in the workpiece with a speed of 20 m/s and scratching distance of 2 nm to emulate the nanometric cutting. The reason that high indentation speed and scratching speed were chosen is to reduce the computation time. After one scratching, the tool tip moves 0.26 nm from the initial position to do another scratching until a machined area of about 1 nm × 2 nm is generated. The bulk temperature is 25°C. The computation time step is 10 fs. In order to observe tool wear clearly, the

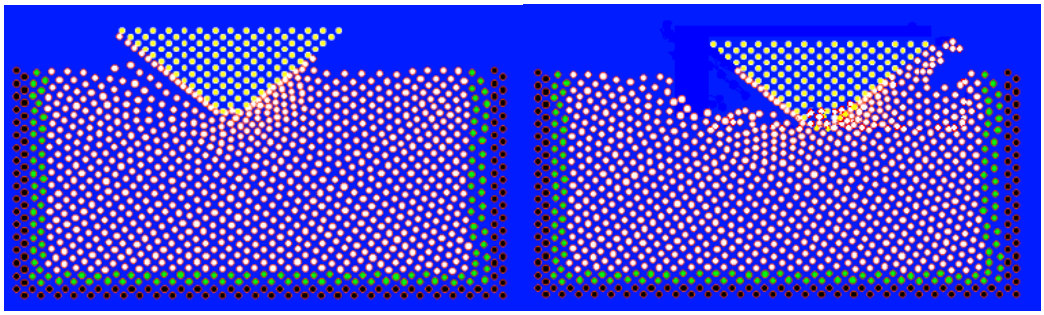

(a) 71.4ps (b) 136 ps

Fig. 2. MD simulation of tool wear.

section diagram of the nanometric cutting is shown in Fig. 2 at two computation times: (a) 71.4 ps, (b) 136 ps. At 71.4 ps, the crystal lattice of the work material begins to be disturbed, and the initiation of micro-dislocations can be observed at each side of the diamond tip in the work material for the reason of releasing the strain energy. At 136 ps, some workpiece atoms move forward to generate the chip. It is a discontinuous atom cluster. There are distinct diffusions between the work atoms and diamond tip atoms at the cutting edge. A few tool atoms separate at the rake face and the cutting edge of the diamond tip, and then move with the chip, while some remain in the workpiece surfaces. This means that the cutting edge of the tool begins to wear. The interference of boundary atoms to the simulation can be ignored since the boundary atoms are outside the cut-off distance of the interactions between silicon atoms and carbon atoms. Fig. 3 shows the simulated images of the AFM diamond tip before and after the cutting respectively. Fig. 3 (b) illustrates that a few diamond tip atoms have been removed from the cutting edge near the rake face and, consequently, an obvious wear flat appears there. This is undesirable because it will produce the unacceptable dimensional or form error on the workpiece and may eventually cause catastrophic failure of the tool [13]. The apex of the AFM diamond tip has been removed, and a little concavity can also be observed on the top of it. It also shows that tool wear has happened.

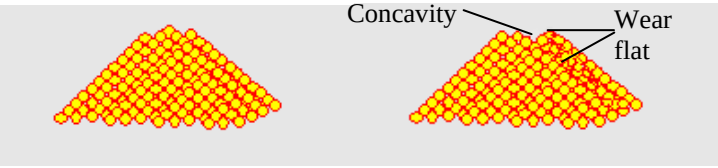

(a) Before cutting (b) After cutting

Fig. 3. Simulation of the tool wear in nanometric cutting.

3.2 The wear mechanism of diamond tip

In the simulation the highest stress in the diamond tip is 6.24 GP. It is lower than the fracture toughness of the diamond. It thus seems that the fracture will not occur. The ratio of the mean tangential cutting force to the mean normal cutting force is 0.54 in this simulation. It shows that strong friction is existing between the workpiece atoms and the diamond tip atoms. The friction and the strain energy released from the deformed crystal lattice will be transformed into cutting heat.

Although some cutting heat will be carried away by the chip, there is still some heat built up at the cutting edge. According to the simulation, the highest local temperature of 813K occurs in the diamond tip and is about 1.43 nm from the apex of the diamond tip.

From Fig. 4 it can be seen that the sublimation energy of carbon atom and silicon atom all decrease with the increase of temperature, but the sublimation energy of carbon decreases much faster than that of the silicon atom. The drastic decrease of sublimation energy and diffusion of the work atoms (as shown in Fig.2. (b)) will weaken the cohesion bond of C-C and make the bond easier to break. The breaking of the C-C bond in the diamond tip will take place at the location where the fewest C-C bond exist. Fig. 5 shows that layers of diamond atoms are removed from the apex and cutting edge of the diamond tip during cutting. The directions of the removal layers are parallel to the (111) plane and (001) plane of the diamond crystal respectively. Fewer C-C bonds exist between the two kinds of crystal planes compared with those of others. It is a typical micro-delamination characteristic in that the diamond atoms are removed in layers and along the direction where the fewest bonds exist. The micro-delaminations result from the high temperature, the atomic diffusion and the drastically decreasing sublimation energy of the carbon atom. The generation of concavity at the apex of diamond tip may be the result of atomic diffusion (as shown in Fig.2. (b)) and the breaking of C-C bond due to the highest temperature concentrating there. The analyses above make it clear that the wear of the diamond tip is caused by thermal effects, atomic diffusion and the drastic decrease of the sublimation energy of carbon atoms in nature. The wear mechanism

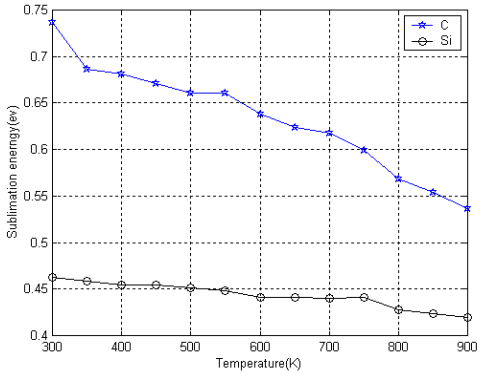

Fig.4. The variation of sublimation energy of C and Si with the temperature.

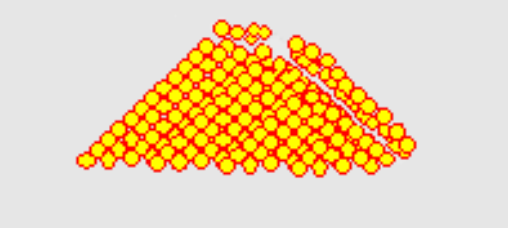

Fig.5. Simulation of the micro-delamination at the diamond tip.

of the diamond tip is consistent with that of the thermo-chemical wear, which can be defined as the wear caused by thermo-chemical effects, such as thermal effects, atomic diffusions, etc. Therefore, thermo-chemical wear can be regarded as the basic wear mechanism of the diamond tip.

In this modeling and simulation, the wear rate is expressed as:

$$W_r = \frac{\Delta V}{F_n l} \tag{7}$$

where ΔV is the wear volume, F_n is the mean normal cutting force, l is the cutting distance. The shear stress causing initial wear is defined as the micro-strength of the diamond tip. Table 1 lists the wear rate and microstrength when the different crystal planes are used as rake face and flank face of the diamond tip. It shows that the (100) plane has the highest microstrength and the lowest wear rate. On the other hand, the (110) plane has the lowest microstrength and the highest wear rate. Therefore, the wear resistance can be characterized by microstrength. The (100) plane is recommended to be used as the rake face and flank face of the diamond cutting tool.

Table 1 The wear rate and microstrength of different crystal plane

	(100)	(111)	(110)
Wear rate (mm^2/Nm)	0.8	1.2	1.9
Microstrength (Gpa)	6.1	5.8	5.4

4. Experimental validation

The nanometric cutting trials are carried out on a single crystal silicon plate by the diamond tip of an AFM (Nanoscope IIIa Dimension 3100, Digital Instruments) in scratching mode. The diamond tip cutting edge radius is 30 nm, and the torque stiffness of the cantilever is 2.9×10^{-5} N/V (as provided by the manufacturer). In the trials, the normal load remains at 80 μN during the indentation and scratching process, and the frequency of the scanning is set at 1 Hz. The scratching process is repeated after the diamond tip indents the surface to some extent until the generation of a machined

surface area of 2 μm by 2 μm. Based on the signal of torque voltage and the stiffness of the cantilever, the tangential cutting force can be calculated as 48.8 μN. The ratio of the tangential cutting force to the normal cutting force is 0.61. The value is quite consistent with that forecasted by the MD simulation as described in section 3.2 ($\frac{0.61-0.54}{0.61}\times 100\% = 11.5\%$ difference).

Fig.6 shows the image of the diamond tip before and after nanometric cutting machining (20

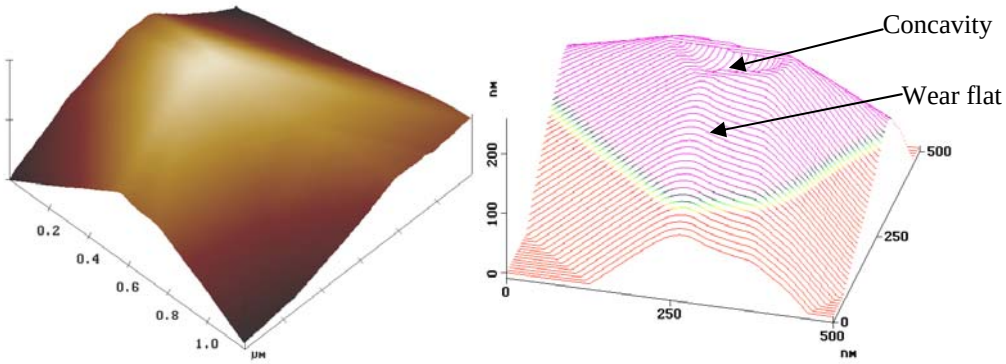

(a) Before machining (b) After machining

Fig. 6. The wear of AFM Diamond tip in nanometric cutting.

times scratching). The obvious wear land and a concavity can be observed as shown in Fig. 6 (b). The result is consistent with that of the MD simulation. It also indicates that the thermo-chemical wear is the basic wear mechanism of the diamond tool.

5. Conclusions

In this paper the wear mechanism of diamond tool in nanometric cutting processes is investigated with the aid of MD simulations and the cutting trials on an AFM. The wear of the diamond tool depends on the cutting temperature, because the cutting heat will decrease the cohesion energy of carbon and weaken the bonding of C-C and thus results in tool wear. The tool wear is characterized by micro-delamination. Thermo-chemical wear is the basic mechanism of the tool wear. The tendency for the diamond tool to micro-delaminate can be characterized by its microstrength. The

(100) plane has the biggest microstrength and the lowest wear rate. The (100) plane is recommended as being the rake face and flank face of the diamond cutting tool.

References:

[1] N. Ikawa, R. R. Donaldson, R. Komanduri, W. König, T. H. Aachen, P. A. Mckeown, T. Moriwaki, I. F. Stowers, Annals of the CIRP, 40 (1997) 587-593.

[2] H. A. Kishawy, M. A. Elbestawi, Proc. Instn. Mech. Engrs., 215 Part B (2001) 755-767.

[3] J. Belak, D. B. Boercker, I. F. Stowers, MRS Bulletin, 18 (1993) 55-60.

[4] N. Ikawa, S. Shimada and H. Tanaka, Nanotechnology, 3 (1992) 6-9.

[5] T. Inamura, N. Takezawa, Y. Kumaki, T. Sata, Annals of the CIRP, 43 (1990) 47-50.

[6] R. Rentsch, in Proceedings of 1st International euspen Conference, Bremen, Germany, 1999, 230-233p.

[7] R. Komanduri, N. Chandrasekaran and L. M. Raff, Wear, 129 (1998) 84-97.

[8] R. Komanduri, N. Chandrasekaran and L. M. Raff, Wear, 240 (2001) 113-143.

[9] K, Maekawa, A. Itoh, Wear, 188 (1995) 115-122.

[10] X. Zhao, B. Bhushan. Wear, 223 (1998) 66-78.

[11] W. G. Hoover, Physical Review, B31(3) (1985) 1695-1697.

[12] M. I. Baskes, Physical Review, B46(5) (1992) 2727-2741.

[13] D. K. Born, W. A. Goodman, Precision Engineering, 25 (2000) 247-257.

Nomenclature

B_i	The bulk modulus, $1/m^3$
$C_p(g)$	The heat capacity at constant pressure of the gaseity, $Wm^{-1}K^{-1}$
$C_p(s)$	The heat capacity at constant pressure of the solid state, $Wm^{-1}K^{-1}$
E_i	The potential of *i*-th atom, J
E_s	The energy per atom of the reference structure, J

E_{sub}	The sublimation energy, J
E_{wti}	The potential of the *i*-th workpiece atom under the action of diamond tip atoms, J
E_{wwi}	The potential of the *i*-th workpiece atom under the action of other workpiece atoms, J
F	A functional of electron density
F_n	The mean normal cutting force, N
F_{ti}	The force acting on the *i*-th diamond tip atom, N
F_{wi}	The force acting on the *i*-th workpiece atom, N
F_{twi}	The force acting on *i*-th diamond tip atom from workpiece atoms, N
F_{tti}	The force acting on the *i*-th diamond tip atoms from other cutting tool atoms, N
F_{wi}	The force acting on the *i*-th workpiece atom, N
l	The cutting distance, m
N_t	The number of diamond tip atoms
N_w	The number of workpiece atoms
R_i^0	The equilibrium nearest-neighbor distance, m
r_{ij}	The distance between atom *i* and atom *j*, m
r_{ti}	The displacement vector of *i*-th diamond tip atoms, m
r_{ttij}	The distance between the *i*-th diamond tip atom and other diamond tip atoms
r_{twij}	The distance between the *i*-th diamond tip atom and workpiece atoms
r_{wti}	The distance between the *i*-th workpiece atom and diamond tip atoms, m
r_{wwij}	The distance between the *i*-th workpiece atom and other workpiece atoms, m
r_{wi}	The displacement vector of *i*-th workpiece atoms, m
Ω_i	The atomic volume of the solid elements, m^3
$\Delta_s^g H(T_1)$	The enthalpy of sublimation at temperature T_1 at standard atmospheric pressure, J
$\Delta_s^g H(T_2)$	The enthalpy of sublimation at temperature T_2 at standard atmospheric pressure, J
ΔV	The wear volume, m^3